

Generation of cold polyatomic cations by cascade reactive two-body ion-atom collisions

Wei-Chen Liang^{1,a}, Feng-Dong Jia^{1,a,*}, Fei Wang², Yu-Han Wang¹, Xi Zhang¹, Jing-Yu Qian¹,

Xiao-Qing Hu³, Yong Wu³, Jian-Guo Wang^{3,†}, Ping Xue^{2,‡} and Zhi-Ping Zhong^{1,§}

¹*School of Physical Sciences, University of Chinese Academy of Sciences, Beijing 100049, China*

²*State Key Laboratory of Low-Dimensional Quantum Physics,*

Department of Physics, Tsinghua University, Beijing 100084, China and

³*Institute of Applied Physics and Computational Mathematics, Beijing 100088, China*

(Dated: August 30, 2023)

We have produced cold (\leq mK) polyatomic cations $^{87}\text{Rb}_N^+$ ($N = 2, 3, \dots, 18$) in the two-step CW-laser photoionization of laser-cooled ^{87}Rb atoms in the ion-atom hybrid trap. The resulting reaction products were directly observed using a combination of time-of-flight mass spectrometry and resonant-excitation mass spectrometry. Furthermore, we experimentally verified the cascade generation and cascade dissociation of this series of polyatomic cations by controlling the duration of ion-atom interaction and the storage times of ions in the ion trap. The methods we developed for assembling and detecting homonuclear polyatomic cations can be applied to any experiment in an ion-atom hybrid trap. This research lays the foundation for studying cold-controlled ion-atom chemistry and the evolution of the interstellar medium, as well as exploring atomically precise metal clusters and physics from a few-body to many-body perspective.

PACS numbers: 34.50.Lf, 34.90.+q, 37.10.Ty, 36.40.Wa, 36.40.-c

Introduction - Charged-neutral cold chemistry becomes one of the frontiers of chemical research, benefited from the development of laser cooling and charged particle trapping technologies[1, 2]. The long-range potential between an ion and an atom is $\propto r^{-4}$ (where r is the internuclear distance between ion and atom) polarization potential[3]. Such a potential is expected to have a large ion-atom interaction cross section[4]. Molecular ions, which can be created in cold ion-atom chemistry[5, 6], offer distinct advantages in terms of their ease of trapping, detection, and possession of additional rotational and vibrational degrees of freedom when compared to atomic ions[7]. Molecular ions are advantageous for research in such areas as cold controlled chemical reaction [1, 5, 8–13], quantum simulation of many-body problems in condensed matter physics[14–16], and quantum information [17]. Cold ion-atom chemistry dominates the evolution of matter in the universe due to the low density and temperatures (on the order of several Kelvin and below) of typical interstellar clouds[2]. The simplest polyatomic molecular ion H_3^+ is the most abundant molecular ion in the universe and plays a key role in interstellar chemistry because it is the start of ion-neutral reactions in the interstellar medium[18]. Polyatomic molecular ions possess more internal complexities compared to diatomic molecular ions, providing unique and novel opportunities in various studies[19]. To date, polyatomic cations that have been created in a lab are not produced by ion-atom collisions and generally have a warm temperature[20–22]. Moreover, as the number of atoms contained increases, polyatomic cations evolve into ion clusters. Clusters and nanomaterials act as links between individual particles and bulk materials, enabling the creation of novel materials with a wide range of potential uses[23, 24]. Utiliz-

ing the continuous variability of atomic composition and atomic number in clusters, clusters can serve as fundamental building blocks for constructing novel materials and devices from the bottom up[23, 24]. The coldest metal clusters are only generated at 0.37 K using helium nanodroplets[25].

Cold ion-atom systems in an ion-atom hybrid trap are a promising platform for studying cold ion-atom interactions and chemical reactions in the mK regime and below [1–3]. Using cold ion-atom hybrid systems, experiments have produced diatomic molecular cations through reactive two-body ion-atom collisions or ion-atom-atom three-body collisions at higher atomic densities[4, 26–35]. These cold diatomic molecular ions experimentally produced are only RbCa^+ [28, 29], RbBa^+ [30], CaYb^+ [27], Ca_2^+ [36], and CaBa^+ [31]. Ion-atom-atom three-body collisions play a role in Rb_2^+ [26, 34], RbBa^+ [33, 35], in which a single ion in a Paul trap was immersed in a cloud of ultracold atoms. The reactive two-body ion-atom collisions are usually explained by the classical Langevin-capture model[37, 38], in which the ion can be atomic or molecular ion. Thus, it can be reasonably inferred that polyatomic cations can be produced in progressive two-body reactive ion-atom collisions, each subsequent reaction occurs based on the reaction products formed in the previous step if there are a sizable number of charged reaction products. According to the principle of microscopic reversibility, the polyatomic cations produced in such a cascade manner may undergo a cascade dissociation. The key of using this approach to prepare polyatomic cations requires creating a sizable number of reactant ions and atoms. CW-photoionization of laser-cooled atoms in an ion-atom hybrid trap may be able to fulfill this requirement. Specifically, in an ion-atom hybrid trap, where the ionic

cloud and atomic cloud spatially overlap, the large ion-atom collision cross-section promises that the co-trapped species can collide at a short-enough range for reactions to proceed. By the way, the polyatomic cations are unlikely to be generated through multi-body non-sequential association in a typical MOT due to the low atomic density in a MOT and the production rate decreases exponentially with the number of contained atoms increases. On the other hand, another challenge is how to detect and identify the reaction products of ion-atom collisions. It was not until 2019 that the direct observation of reactants, intermediates, and products via ionization spectroscopy has been achieved by Hu *et al.*[39].

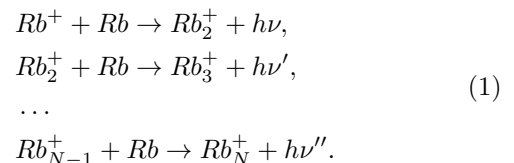
Here, we report the creation of a series of polyatomic cations $^{87}\text{Rb}_N^+$ ($N = 2, 3, \dots, 18$) in CW-laser photoionization of cold ^{87}Rb atoms in an ion-atom hybrid trap. We used the combination of TOF mass spectrometry and REMS to discriminate these reaction products and directly observed the production of a large number ($\sim 10^6$ $^{87}\text{Rb}_N^+$, $N = 2, 3, \dots, 7$) of polyatomic cations $^{87}\text{Rb}_N^+$ ($N = 2, 3, \dots, 18$) as reaction products. Moreover, by changing the interaction time of ion-atom collisions and the storage time of ions in the ion trap, we observed a cascade generation from diatomic cations to polyatomic cations and the cascade dissociation of polyatomic cations.

Experimental Setup - An $^{87}\text{Rb}^+$ - ^{87}Rb hybrid trap is used in our experiments. A detailed description of this apparatus can be found in our previous study[40]. In brief, the apparatus comprises an Rb standard magneto-optical trap (MOT) and a mass-selective linear Paul trap (LPT), the LPT consists of a quadrupole arrangement of four central parallel radio-frequency (RF) rods and two DC hollow end-cap ring electrodes positioned along the cylindrical axis. Both the MOT and the LPT are spatially concentric and combined in a polyhedral non-magnetic stainless-steel cavity. The number of atoms and the $1/e^2$ half-waist of the cold atomic cloud in the MOT were measured as $\sim 10^8$ and ~ 1.0 mm, respectively using absorption imaging. The temperature of cold atoms was approximately 0.2 mK. $^{87}\text{Rb}^+$ ions were produced through two-step CW-laser photoionization of cold ^{87}Rb atoms. Here the MOT cooling/trapping beams served as the first excitation laser with a detuning of -12 MHz of the transition $5\ ^2S_{1/2}, F = 2 \rightarrow 5\ ^2P_{3/2}, F' = 3$. A CW-diode laser served as the second excitation laser, i.e., the ionizing laser, which photoionizes the ^{87}Rb atoms in the $5P_{3/2}$ states, the wavelength and intensity of the ionizing laser were 478.8 nm and 265.25 mW/cm² in this work. The LPT had a well-depth of ~ 0.7 eV, corresponding to a maximum temperature of $10^3 - 10^4$ K for the trapped $^{87}\text{Rb}^+$ [40, 41]. The trap was operated at a radio-frequency (RF) of $\Omega_{\text{trap}} = 2\pi \times 550$ kHz with an amplitude of $V_{\text{trap}} = 140$ V. The radial directions x, y, and axial direction z of the trapped ionic cloud were 2.3, 2.3, and 20.2 mm, respectively[41] and $\sim 10^7$ ions were trapped in the LPT[42]. An additional RF with an ampli-

tude of $V_{\text{RF}} = 4$ V can be applied to the quadrupole electrodes. When the voltage on the end-cap ring electrode closer to the microchannel plate (MCP) were turned off, this caused the trapped ions to be pushed towards the MCP, and the resulting TOF spectrum was recorded using an oscilloscope.

The experimental errors in this work resulted from the following factors: the systematic error from the fluctuation of temperature and number of cold atoms of approximately 10-15%, the error resulting from the deconvoluting procedure, the statistical uncertainties, the uncertainties in determining the ionizing-laser intensity of approximately 1-5%, and the uncertainty caused by 1 MHz linewidth of the ionizing laser with the wavelength 478.8 nm.

Results - Our experiments begin with the preparation of a mixture of cold ^{87}Rb atoms and $^{87}\text{Rb}^+$ ions. We first loaded the MOT to a steady state, and then the ionizing laser and the LPT were simultaneously switched on. The MOT, the ionizing laser, and the LPT worked together for an adjustable period T_{rec} . Then the MOT, the ionizing laser as well as the LPT were switched off, and a TOF spectrum was obtained. An ion-atom mixture was created during the photoionization of cold ^{87}Rb atoms. The experimental sequence is depicted in Fig.1. There are two types of TOF spectra that we measured, as shown in Fig.2(a). One displays a single broad peak measured at the reaction time of $T_{\text{rec}} = 100$ ms. Another has two distinct peaks measured at the reaction time of $T_{\text{rec}} = 750$ ms, i.e., a broad peak (peak 2) alongside the strong $^{87}\text{Rb}^+$ peak (peak 1), the peak 2 means that the formation of $^{87}\text{Rb}_N^+$ as the reaction products in the $^{87}\text{Rb}^+$ - ^{87}Rb collisions. As discussed above, a series of polyatomic species occur in a cascading manner deduced from Langevin capture model[37, 38], which is represented by the following equations,



The relative ion intensity measured by the MCP was converted into absolute ion number by combining atomic absorption imaging and rate equations, which has used in our previous work[42]. The intensity, position, and half-width for a peak in a TOF spectrum were derived by fitting with the probability density function of the Gumbel distribution[42]. Notably, the spectrum is limited to detecting only two peaks, even though there is a possibility of multiple polyatomic cations being present. It may be attributed to the significant overlap of multiple peaks. Therefore, it is necessary to develop method that can effectively discriminate between different reaction products.

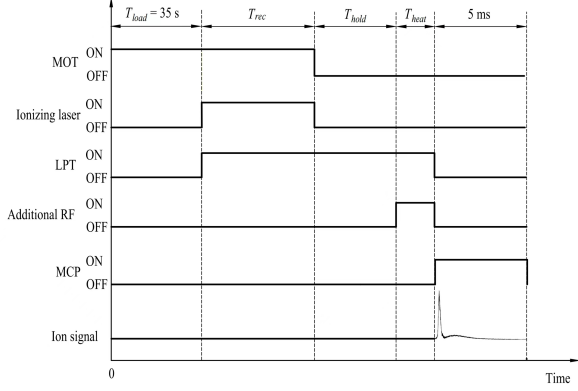


FIG. 1. The present experimental sequence diagram for the detection methods.

We investigated the evolution of the total number of ions and the number of reaction products (peak 2) as a function of hold time in the LPT. Measurements were taken after the reaction time of $T_{\text{rec}} = 750 \text{ ms}$. Then, the MOT and ionizing laser were turned off, while the LPT remained active for an adjustable period of T_{hold} . At the end of this period, a TOF spectrum was obtained. The experimental sequence is depicted in Fig.1. As depicted in Fig.2(b), both the total number of ions and the number of reaction products can be well-fitted with a single exponential function. Moreover, the rate of decrease in the number of reaction products is faster than that of the total number of ions. There are two mechanisms that result in the loss of ions in the LPT. One is the limited trapping capability of the LPT leads to a decrease in the number of ions in the LPT. Another is the dissociation of a molecular ion. Molecular ions ultimately dissociate into atomic ions, hence the decreasing total ion count reflects the the limited trapping capability of the LPT. On the other hand, the decay of reaction product molecular ions is faster due to their dissociation.

The primary factor influencing ion-atom collisions is the collision energy, which refers to the relative kinetic energy between reactant ions and atoms. To determine the collision energy, we begin our analysis by examining the temperature of atoms and ions. The temperature of the MOT atom is $\sim 0.2 \text{ mK}$ for ^{87}Rb . The ions in the MOT and those stored in the LPT exhibit significantly different temperatures (i.e., kinetic energy). Based on energy and momentum conservation principles, the initial temperature of $^{87}\text{Rb}^+$ ions generated by the photoionization of cold atoms is estimated to be a few mK. And the temperature for the trapped $^{87}\text{Rb}^+$ in the LPT is approximately $10^3 \sim 10^4 \text{ K}$ as the LPT's well-depth is approximately 0.7 eV [41]. Therefore, the collision energy is determined by the ion kinetic energy. To deter-

mine whether ions in the LPT contribute to ion-atom reaction collisions, we have designed the following experimental scheme. Measurements were taken after the reaction time of $T_{\text{rec}} = 500 \text{ ms}$, then, the ionizing laser was turned off, and the intensity of the peak 2 is measured as a function of the hold time T_{hold} in the LPT in both cases where MOT is turned on or off. In both cases, the intensity of peak 2 is approximately the same shown in Fig.2(c). It means that the ions in the LPT almost do not react with atoms. Therefore, the collision energy between $^{87}\text{Rb}^+$ - ^{87}Rb collisions approximates the kinetic energy of $^{87}\text{Rb}^+$ ions in the MOT. Moreover, we can control the occurrence and cessation of ion-atom collisions by controlling the switch of the MOT and the ionizing laser. According to the fitting of experimental data with rate equations[43], the diffusion rate of $^{87}\text{Rb}^+$ ions in the MOT is approximately $1.0/\text{s}$, corresponding to a temperature of $\sim 5.2 \text{ mK}$. Moreover, the collision energy is not entirely converted into the kinetic energy of the reaction products. Therefore, in this study, the collision energy of ion-atom reactions lies in the range of a few mK.

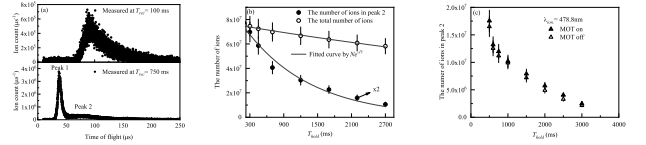


FIG. 2. (a) Two typical TOF spectra using TOF mass spectrometry without additional RF. The solid line represents the measurement taken at the reaction time of $T_{\text{rec}} = 750 \text{ ms}$, while the dashed line represents the measurement taken at the reaction time of $T_{\text{rec}} = 100 \text{ ms}$. (b) The number of the total ion and ions in peak 2 as a function of the hold time T_{hold} . (c) The intensity of peak 2 was measured as a function of T_{hold} with or without the presence of cold atoms, and the reaction time of $T_{\text{rec}} = 500 \text{ ms}$.

Now we aim to directly observe these reaction products. As discussed above, conventional TOF mass spectrometry cannot discriminate between different reaction products. We have employed two approaches, combining TOF spectrometry with REMS, to directly observe these reaction products.

By altering the intensity ratio in an apparently isolated peak formed by strong overlapping of multiple peaks, particularly by quenching the signal with higher intensity, the peak may be decomposed into these multiple peaks. To quench unwanted ions in the LPT, the work in Ref.[44, 45] demonstrates that mass selective resonant excitation can be employed by applying an additional RF. When the frequency of the additional RF matches the radial secular frequency ω_r of a particular ion species, the ions absorb the RF energy and exit the LPT. The theoretical ω_r for $^{87}\text{Rb}_N^+$ can be calculated as $\omega_r(^{87}\text{Rb}_N^+) = 2\pi \times 109.2/N \text{ kHz}$ using the Mathieu equations[46]. In our study, the strong signal of $^{87}\text{Rb}_2^+$ was quenched by

applying an additional RF with $\Omega_{RF} = 2\pi \times 58.4$ kHz, which is close to the theoretical value $2\pi \times 109.2/2 = 2\pi \times 54.6$ kHz. The experimental procedure is shown in Fig.1, here, $T_{rec} = 350$ ms, $T_{hold} = 0$ ms and $T_{heat} = 50$ μ s. As depicted in Fig.3(a), the broad peak 2 splits into six distinguishable narrow peaks. By comparing the time-of-flight ratios of these peaks with the squared mass ratio of $^{87}\text{Rb}_N^+$, we readily identify these peaks as $^{87}\text{Rb}_2^+$, $^{87}\text{Rb}_3^+$, $^{87}\text{Rb}_4^+$, $^{87}\text{Rb}_5^+$, $^{87}\text{Rb}_6^+$, and $^{87}\text{Rb}_7^+$. The magnitude of these ions is about 10^6 , a sufficiently large value to enable cascade reactions. The reason why $^{87}\text{Rb}_2^+$ does not disappear may be the existence of the second harmonic frequency and ions in the MOT are not governed by the dynamics of the LPT. As the value of N in $^{87}\text{Rb}_N^+$ increases, the width of the corresponding peak broadens and the intensity diminishes. Molecular ions $^{87}\text{Rb}_N^+$ with $N \geq 7$ cannot be distinguished in the TOF spectrum. To observe these polyatomic cations containing more than seven atoms, we combine REMS with TOF mass spectrometry, each experimental cycle is shown in Fig.1. By repeating this cycle for different frequencies of the additional RF, we obtained the total number of ions as a function of the additional RF frequency, known as REMS. When the RF frequency resonated with the ω_r of an ion species in the LPT, it caused a reduction in the total number of ions, resulting in a dip in the measured REMS. It is important to note that we used TOF spectrum instead of measuring the fluorescence of reactant ions, as done in previous studies[28–30, 47, 48]. As shown in Fig.3(b), we can clearly see the production of polyatomic cations $^{87}\text{Rb}_N^+$ ($N = 2, 3, \dots, 18$) by comparing with theoretical radial secular frequencies. Since the interaction between the trapped ions in the LPT perturbs their radial secular motion[49, 50], the position of an experimental dip and its corresponding theoretical value are not entirely consistent. Besides, there are many dips that correspond to the second harmonic frequencies of a particular ion species, as shown in Fig.3(b). This is due to that the additional RF can have the side effect of heating the ions[49, 51].

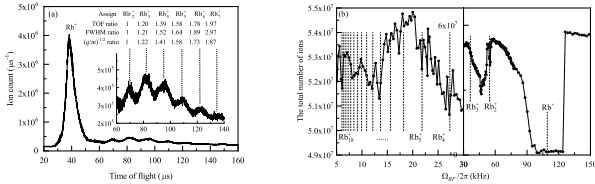


FIG. 3. Direct detection of reaction products. (a) Measurements were carried out at the reaction time of $T_{rec} = 350$ ms, $T_{hold} = 0$ ms and $T_{heat} = 50$ μ s. The additional RF had a frequency $\Omega_{RF} = 2\pi \times 58.4$ kHz. (b) REMS combined with TOF mass spectrometry measured at the reaction time $T_{rec} = 750$ ms, $T_{hold} = 0$ ms and $T_{heat} = 1$ ms. The amplitude of the additional RF was $V_{RF} = 4$ V. The dashed lines represent the theoretical radial secular frequencies ω_r of $^{87}\text{Rb}_N^+$.

Now we aim to experimentally validate the production and dissociation of polyatomic cations in a cascade manner, as predicted by the classical Langevin-capture model[37, 38]. In a cascade production process, the production time of polyatomic cations is expected to increase as the number of atoms contained increases. Polyatomic cations would sequential dissociation, and the polyatomic cation containing k atoms initially break down into the polyatomic cation containing $k - 1$ atoms.

To validate the cascade production characteristics of these reaction products $^{87}\text{Rb}_N^+$ ($N = 2, 4, \dots$), we varied the reaction time T_{rec} and measured the REMS at each specific T_{rec} , we can observe the emergence of $^{87}\text{Rb}_N^+$ as the reaction progressed. Fig.4(a) and (b) display REMS at the reaction times of 90 ms, 100 ms, and 105 ms, respectively. Notably, as shown in Fig.4(a), at a reaction time of 90 ms, no observable dip signal was detected within the excitation frequency range of 5~80 kHz. However, at the reaction time of 100 ms, a broad dip signal near the resonant frequency of $^{87}\text{Rb}_2^+$ was observed, indicating the production of $^{87}\text{Rb}_2^+$. As the reaction time increased to 105 ms, shown in Fig.4(b), the dip signal progressed toward lower extra excitation frequencies, indicating the production of molecular ions with an increased number of atoms. This indicates the generation of $^{87}\text{Rb}_2^+$ and $^{87}\text{Rb}_N^+$ ($N = 3, 4, \dots, 17$) occurs sequentially according to the theoretical radial secular frequency $\omega_r = 2\pi \times 109.2/N$ kHz of $^{87}\text{Rb}_N^+$. Dip signals without markers in Fig.4 represented the second harmonic frequencies of polyatomic cations. Additionally, each signal of polyatomic cations exhibited varying intensities, indicating that geometric structural stabilities could play a significant role, which requires further investigations.

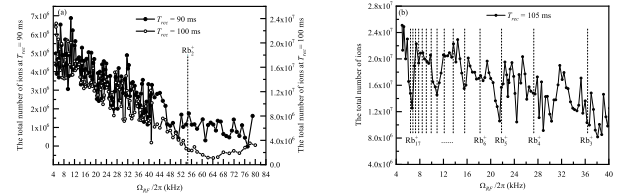


FIG. 4. Cascade feature for the generation of the reaction products $^{87}\text{Rb}_N^+$ in the $^{87}\text{Rb}^+ - ^{87}\text{Rb}$ collisions. The additional RF with amplitude $V_{RF} = 4$ V was applied and $T_{hold} = 0$ ms. The vertical dashed lines in the figures represent the theoretical radial secular frequency ω_r of $^{87}\text{Rb}_N^+$. (a) Comparison between REMS measured at $T_{rec} = 90$ ms and $T_{rec} = 100$ ms. (b) REMS measured at $T_{rec} = 105$ ms.

To investigation of the dissociation path of polyatomic molecules, we measured a series of REMS with different storage time T_{hold} of ions in the LPT. Fig.5(a), at the hold time $T_{hold} = 0$ ms, the dip formed by molecular ions containing 18 atoms is clearly visible. As the hold time T_{hold} in the LPT increased, some polyatomic cations disappeared while the signals of others with smaller num-

bers of atoms became intensified. For example, at the hold time $T_{hold} = 200$ ms, the signal of $^{87}\text{Rb}_{18}^+$ vanished, while the signals of $^{87}\text{Rb}_{15}^+$ and $^{87}\text{Rb}_{17}^+$ became clearer. As the hold time T_{hold} increased to 300 ms, the signals of heavy polyatomic cations $^{87}\text{Rb}_{15}^+$ and $^{87}\text{Rb}_{17}^+$ weakened, while the signals of lighter polyatomic cations like $^{87}\text{Rb}_8^+$ became more prominent, shown in Fig.5(b). Additionally, the second harmonic frequency signals of polyatomic cations also evolved, as evident in the signal of $^{87}\text{Rb}_{11}^+$, which appeared at the hold time $T_{hold} = 200$ ms and disappeared at the hold time $T_{hold} = 300$ ms. These findings indicate a cascade dissociation process, in the 0-200 ms hold time, $^{87}\text{Rb}_{18}^+$, $^{87}\text{Rb}_{17}^+$, $^{87}\text{Rb}_{16}^+$ gradually dissociate into $^{87}\text{Rb}_{17}^+$, $^{87}\text{Rb}_{16}^+$, $^{87}\text{Rb}_{15}^+$, respectively, then when the hold time comes to 300 ms, the signals of heavy polyatomic cations such as $^{87}\text{Rb}_{17}^+$ and $^{87}\text{Rb}_{11}^+$ gradually disappear and only the signals of lighter polyatomic cations remain.

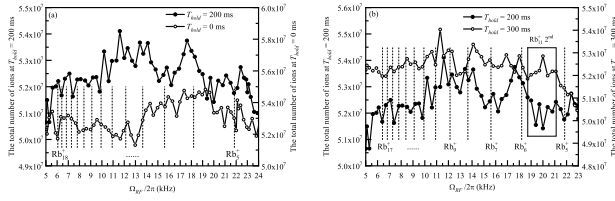


FIG. 5. Cascade feature for the dissociation processes of reaction products $^{87}\text{Rb}_N^+$ in the $^{87}\text{Rb}^+ - ^{87}\text{Rb}$ collisions. The reaction time T_{rec} was 750 ms and $T_{heat} = 1$ ms. The additional RF with amplitude $V_{RF} = 4$ V was applied. The vertical dashed lines represent the theoretical radial secular frequencies ω_r of $^{87}\text{Rb}_N^+$ and the box illustrates the second harmonic frequency of $^{87}\text{Rb}_{11}^+$ as an example of non-resonant signals. (a) Comparison between REMS measured at $T_{hold} = 0$ ms and $T_{hold} = 200$ ms. (b) Comparison between the REMS measured at $T_{hold} = 200$ ms and $T_{hold} = 300$ ms.

Conclusion - In summary, a significant abundance of cold polyatomic cations, denoted as $^{87}\text{Rb}_N^+$ ($N = 2, 3, \dots, 18$), was successfully generated within an $^{87}\text{Rb} - ^{87}\text{Rb}^+$ mixture. This mixture was created through a two-step CW-laser photoionization process of laser-cooled ^{87}Rb atoms in an ion-atom hybrid trap. The formation of these polyatomic cations occurred by progressive two-body reactive ion-atom collisions, i.e., cascade two-body ion-atom collisions, which is deduced by the Langevin-capture model[37, 38]. The collision energy of ion-atom collisions is estimated not to be higher than millikelvin magnitudes since the kinetic energy of the atomic ions produced during the photoionization of laser-cooled ^{87}Rb atoms inherits from their parent atoms. We have developed two approaches to directly observe these reaction products by applying an additional RF. The first method involves using an additional RF signal with a fixed frequency to suppress the intense signal of $^{87}\text{Rb}_2^+$, thereby dividing the seemingly isolated peak formed by these re-

action products into multiple distinguishable peaks. The second method involves measuring the overall quantity of ions using TOF mass spectrometry while varying the frequency of the additional RF. Furthermore, our investigation demonstrated the occurrence of cascade reactions leading to the formation of a series of polyatomic cations $^{87}\text{Rb}_N^+$ ($N = 2, 3, \dots, 18$), with distinct cascade features evident within the associated dissociation processes. Our findings offer comprehensive insights into the dynamics of cold ion-atom interactions and chemical reactions. Benefiting from rich degrees of freedom, these polyatomic species play significant roles in precision measurement and quantum information sciences. Additionally, this series of polyatomic cations forms an atomically precise metal cluster, which holds significant importance in the study of physics from few-body to many-body perspectives.

The authors express their deep appreciation of Dr. Xin-Yu Luo (Max-Planck-Institute for Quantum Optics) and Prof. Zhen-Sheng Yuan (University of Science and Technology of China) for our fruitful discussions.

This study was supported by the National Key Research and Development Program of China (Grant Nos. 2017YFA0402300 and 2017YFA0304900), the Beijing Natural Science Foundation (Grant No. 1212014), Fundamental Research Funds for the Central Universities, the Strategic Priority Research Program (Grant No. XDB28000000) of the Chinese Academy of Sciences., specialized research fund for CAS Key Laboratory of Geospace Environment (Grant No. GE2020-01), and National Natural Science Foundation of China (Grant Nos. 61975091, 61575108).

* ^aThese authors have contributed equally to this work.

† wang_jianguo@iapcm.ac.cn

‡ xuep@tsinghua.edu.cn

§ zpzhong@ucas.ac.cn

- [1] P. Puri, M. Mills, I. Simbotin, J. A. Montgomery, R. Ct, C. Schneider, A. G. Suits, and E. R. Hudson, *Nature Chemistry* **11**, 615 (2019), ISSN 1755-4330, 1755-4349, URL <http://www.nature.com/articles/s41557-019-0264-3>.
- [2] B. R. Heazlewood and T. P. Softley, *Nature Reviews Chemistry* **5**, 125 (2021), ISSN 2397-3358, URL <http://www.nature.com/articles/s41570-020-00239-0>.
- [3] M. Tomza, K. Jachymski, R. Gerritsma, A. Negretti, T. Calarco, Z. Idziaszek, and P. S. Julienne, *Reviews of Modern Physics* **91**, 035001 (2019), ISSN 0034-6861, 1539-0756, URL <https://link.aps.org/doi/10.1103/RevModPhys.91.035001>.
- [4] A. Krkow, A. Mohammadi, A. Hrter, and J. Hecker Denschlag, *Physical Review A* **94**, 030701 (2016), ISSN 2469-9926, 2469-9934, URL <https://link.aps.org/doi/10.1103/PhysRevA.94.030701>.
- [5] M. Tomza, *Phys. Rev. Lett.* **115**, 063201 (2015), URL <https://link.aps.org/doi/10.1103/PhysRevLett.>

- 115.063201.
- [6] H. da Silva Jr, M. Raoult, M. Aymar, and O. Dulieu, *New Journal of Physics* **17**, 045015 (2015), URL <https://dx.doi.org/10.1088/1367-2630/17/4/045015>.
 - [7] M. miakowski and M. Tomza, *Physical Review A* **101**, 012501 (2020), ISSN 2469-9926, 2469-9934, URL <https://link.aps.org/doi/10.1103/PhysRevA.101.012501>.
 - [8] J. Deiglmayr, A. Göritz, T. Best, M. Weidemüller, and R. Wester, *Phys. Rev. A* **86**, 043438 (2012), URL <https://link.aps.org/doi/10.1103/PhysRevA.86.043438>.
 - [9] P. Puri, M. Mills, C. Schneider, I. Simbotin, J. A. Montgomery, R. Ct, A. G. Suits, and E. R. Hudson, *Science* **357**, 1370 (2017), <https://www.science.org/doi/pdf/10.1126/science.aan4701>, URL <https://www.science.org/doi/abs/10.1126/science.aan4701>.
 - [10] A. Kilaj, H. Gao, D. Rsch, U. Rivero, J. Kpper, and S. Willitsch, *Nature Communications* **9**, 2096 (2018), ISSN 2041-1723, URL <https://www.nature.com/articles/s41467-018-04483-3>.
 - [11] M. Tomza, *Phys. Chem. Chem. Phys.* **19**, 16512 (2017), publisher: The Royal Society of Chemistry, URL <http://dx.doi.org/10.1039/C7CP02127E>.
 - [12] A. D. Drfler, P. Eberle, D. Koner, M. Tomza, M. Meuwly, and S. Willitsch, *Nature Communications* **10**, 5429 (2019), ISSN 2041-1723, URL <https://www.nature.com/articles/s41467-019-13218-x>.
 - [13] M. Kas, J. Loreau, J. Liévin, and N. Vaeck, *Phys. Rev. A* **99**, 042702 (2019), URL <https://link.aps.org/doi/10.1103/PhysRevA.99.042702>.
 - [14] R. Côté, *Phys. Rev. Lett.* **85**, 5316 (2000), URL <https://link.aps.org/doi/10.1103/PhysRevLett.85.5316>.
 - [15] W. Casteels, J. Tempere, and J. T. Devreese, *Journal of Low Temperature Physics* **162**, 266 (2011), ISSN 0022-2291, 1573-7357, URL <http://link.springer.com/10.1007/s10909-010-0286-0>.
 - [16] U. Bissbort, D. Cocks, A. Negretti, Z. Idziaszek, T. Calarco, F. Schmidt-Kaler, W. Hofstetter, and R. Gerritsma, *Phys. Rev. Lett.* **111**, 080501 (2013), URL <https://link.aps.org/doi/10.1103/PhysRevLett.111.080501>.
 - [17] H. Doerk, Z. Idziaszek, and T. Calarco, *Phys. Rev. A* **81**, 012708 (2010), URL <https://link.aps.org/doi/10.1103/PhysRevA.81.012708>.
 - [18] T. R. Geballe and T. Oka, *Science* **312**, 1610 (2006), ISSN 0036-8075, 1095-9203, URL <https://www.science.org/doi/10.1126/science.1126279>.
 - [19] X.-Y. Chen, S. Biswas, S. Eppelt, A. Schindewolf, F. Deng, T. Shi, S. Yi, T. A. Hilker, I. Bloch, and X.-Y. Luo, *Ultracold field-linked tetratomic molecules* (2023), arXiv: 2306.00962.
 - [20] M. E. Jacox, *Journal of Physical and Chemical Reference Data* **32**, 1 (2003), ISSN 0047-2689, URL <https://doi.org/10.1063/1.1497629>.
 - [21] I. Boustani, *Alkali Metal Clusters* (Springer International Publishing, Cham, 2020), pp. 69–111, ISBN 978-3-030-32726-2, URL https://doi.org/10.1007/978-3-030-32726-2_3.
 - [22] C. Brchignac, P. Cahuzac, B. Concina, J. Leygnier, and I. Tignres, *The European Physical Journal D* **12**, 185 (2000), ISSN 14346060, URL <http://link.springer.com/10.1007/s100530070056>.
 - [23] W. A. de Heer, *Rev. Mod. Phys.* **65**, 611 (1993), URL <https://link.aps.org/doi/10.1103/RevModPhys.65.611>.
 - [24] G. Y. L. Z.-F. Z. Ji-Jun, *PHYSICS* **51**, 550 (2022), ISSN 0379-4148, URL <https://wuli.iphy.ac.cn/article/doi/10.7693/wl20220807>.
 - [25] J. Tiggesbunker and F. Stienkemeier, *Phys. Chem. Chem. Phys.* **9**, 4748 (2007), URL <http://dx.doi.org/10.1039/B703575F>.
 - [26] T. Dieterle, M. Berngruber, C. Hlzl, R. Lw, K. Jachymski, T. Pfau, and F. Meinert, *Physical Review Letters* **126**, 033401 (2021), ISSN 0031-9007, 1079-7114, URL <https://link.aps.org/doi/10.1103/PhysRevLett.126.033401>.
 - [27] W. G. Rellergert, S. T. Sullivan, S. Kotochigova, A. Petrov, K. Chen, S. J. Schowalter, and E. R. Hudson, *Physical Review Letters* **107**, 243201 (2011), ISSN 0031-9007, 1079-7114, URL <https://link.aps.org/doi/10.1103/PhysRevLett.107.243201>.
 - [28] F. H. J. Hall, M. Aymar, N. Bouloufa-Maafa, O. Dulieu, and S. Willitsch, *Physical Review Letters* **107**, 243202 (2011), ISSN 0031-9007, 1079-7114, URL <https://link.aps.org/doi/10.1103/PhysRevLett.107.243202>.
 - [29] F. H. J. Hall, P. Eberle, G. Hegi, M. Raoult, M. Aymar, O. Dulieu, and S. Willitsch, *Molecular Physics* **111**, 2020 (2013), ISSN 0026-8976, 1362-3028, arXiv:1302.4682 [physics].
 - [30] F. H. Hall, M. Aymar, M. Raoult, O. Dulieu, and S. Willitsch, *Molecular Physics* **111**, 1683 (2013), ISSN 0026-8976, 1362-3028, URL <https://www.tandfonline.com/doi/full/10.1080/00268976.2013.770930>.
 - [31] S. T. Sullivan, W. G. Rellergert, S. Kotochigova, and E. R. Hudson, *Physical Review Letters* **109**, 223002 (2012), ISSN 0031-9007, 1079-7114, URL <https://link.aps.org/doi/10.1103/PhysRevLett.109.223002>.
 - [32] A. Hrter, A. Krkow, A. Brunner, W. Schnitzler, S. Schmid, and J. H. Denschlag, *Physical Review Letters* **109**, 123201 (2012), ISSN 0031-9007, 1079-7114, URL <https://link.aps.org/doi/10.1103/PhysRevLett.109.123201>.
 - [33] A. Krkow, A. Mohammadi, A. Hrter, J. H. Denschlag, J. Prez-Ros, and C. H. Greene, *Physical Review Letters* **116**, 193201 (2016), ISSN 0031-9007, 1079-7114, URL <https://link.aps.org/doi/10.1103/PhysRevLett.116.193201>.
 - [34] T. Dieterle, M. Berngruber, C. Hlzl, R. Lw, K. Jachymski, T. Pfau, and F. Meinert, *Physical Review A* **102**, 041301 (2020), ISSN 2469-9926, 2469-9934, URL <https://link.aps.org/doi/10.1103/PhysRevA.102.041301>.
 - [35] A. Mohammadi, A. Krkow, A. Mahdian, M. Dei, J. Prez-Ros, H. da Silva, M. Raoult, O. Dulieu, and J. Hecker Denschlag, *Physical Review Research* **3**, 013196 (2021), ISSN 2643-1564, URL <https://link.aps.org/doi/10.1103/PhysRevResearch.3.013196>.
 - [36] S. T. Sullivan, W. G. Rellergert, S. Kotochigova, K. Chen, S. J. Schowalter, and E. R. Hudson, *Phys. Chem. Chem. Phys.* **13**, 18859 (2011), URL <http://dx.doi.org/10.1039/C1CP21205B>.
 - [37] M. P. Langevin, *Annales de Chimie et de Physique* **5**, 245 (1905).
 - [38] R. D. Levine, *Molecular Reaction Dynamics* (Cambridge University Press, 2009).
 - [39] M.-G. Hu, Y. Liu, D. D. Grimes, Y.-W. Lin, A. H. Gheorghe, R. Vexiau, N. Bouloufa-Maafa, O. Dulieu, T. Rosenband, and K.-K. Ni, *Science* **366**, 1111 (2019), ISSN 0036-8075, 1095-9203, URL <https://www>.

- science.org/doi/10.1126/science.aay9531.
- [40] S.-F. Lv, F.-D. Jia, J.-Y. Liu, X.-Y. Xu, P. Xue, and Z.-P. Zhong, Chinese Physics Letters **34**, 013401 (2017), ISSN 0256-307X, 1741-3540, URL <https://iopscience.iop.org/article/10.1088/0256-307X/34/1/013401>.
 - [41] X.-K. Li, D.-C. Zhang, S.-F. Lv, J.-Y. Liu, F.-D. Jia, Y. Wu, X.-H. Lin, R. Li, X.-Y. Xu, P. Xue, et al., Journal of Physics B: Atomic, Molecular and Optical Physics **53**, 219501 (2020), ISSN 0953-4075, 1361-6455, URL <https://iopscience.iop.org/article/10.1088/1361-6455/abb259>.
 - [42] W.-C. Liang, Y.-H. Wang, X. Zhang, F. Wang, F.-D. Jia, P. Xue, and Z.-P. Zhong, Acta Physica Sinica **72**, 093401 (2023).
 - [43] W.-C. Liang, F.-D. Jia, F. Wang, X. Zhang, Y.-H. Wang, J.-Y. Qian, J.-Y. Zhou, Y. Wu, J.-G. Wang, P. Xue, et al., *Reactive ion-atom collisions in cw-laser photoionization of laser-cooled rb atoms* (2023), arXiv: 2303.10360v1.
 - [44] A. Drakoudis, M. Sllner, and G. Werth, International Journal of Mass Spectrometry **252**, 61 (2006), ISSN 1387-3806, URL <https://www.sciencedirect.com/science/article/pii/S1387380606001047>.
 - [45] H. A. Schuessler, E. N. Fortson, and H. G. Dehmelt, Phys. Rev. **187**, 5 (1969), URL <https://link.aps.org/doi/10.1103/PhysRev.187.5>.
 - [46] W. Paul, Rev. Mod. Phys. **62**, 531 (1990), URL <https://link.aps.org/doi/10.1103/RevModPhys.62.531>.
 - [47] F. H. J. Hall and S. Willitsch, Physical Review Letters **109**, 233202 (2012), ISSN 0031-9007, 1079-7114, URL <https://link.aps.org/doi/10.1103/PhysRevLett.109.233202>.
 - [48] B. Roth, P. Blythe, and S. Schiller, Phys. Rev. A **75**, 023402 (2007), URL <https://link.aps.org/doi/10.1103/PhysRevA.75.023402>.
 - [49] D. S. Goodman, I. Sivarajah, J. E. Wells, F. A. Narducci, and W. W. Smith, Phys. Rev. A **86**, 033408 (2012), URL <https://link.aps.org/doi/10.1103/PhysRevA.86.033408>.
 - [50] R. Blümel, C. Kappler, W. Quint, and H. Walther, Phys. Rev. A **40**, 808 (1989), URL <https://link.aps.org/doi/10.1103/PhysRevA.40.808>.
 - [51] I. Sivarajah, D. S. Goodman, J. E. Wells, F. A. Narducci, and W. W. Smith, Phys. Rev. A **86**, 063419 (2012), URL <https://link.aps.org/doi/10.1103/PhysRevA.86.063419>.